Bioconjugate Chemistry

ARTICLE

pubs.acs.org/bc

Inflammation Responsive Logic Gate Nanoparticles for the Delivery of Proteins

Enas A. Mahmoud,[†] Jagadis Sankaranarayanan,[†] José M. Morachis,[†] Gloria Kim,[†] and Adah Almutairi*[,†,‡,§]

[†]Skaggs School of Pharmacy and Pharmaceutical Sciences, [‡]Materials Science and Engineering, and [§]NanoEngineering, University of California at San Diego, La Jolla, California 92093-0657, United States

Supporting Information

ABSTRACT: Oxidative stress and reduced pH are important stimuli targets for intracellular delivery and for delivery to diseased tissue. However, there is a dearth of materials able to deliver bioactive agents selectively under these conditions. We employed our recently developed dual response strategy to build a polymeric nanoparticle that degrades upon exposure to two stimuli in tandem. Our polythioether ketal based nanoparticles undergo two chemical transformations; the first is the oxidation of the thioether groups along the polymer backbone of the nanoparticles upon exposure to reactive oxygen species (ROS). This transformation switches the polymeric backbone from hydrophobic to hydrophilic and thus allows, in mildly acidic environments, the rapid acid-catalyzed degradation of the ketal groups also along the polymer backbone. Dynamic light scattering and payload release studies showed full particle degradation only in conditions that combined both oxidative stress and acidity, and these conditions led to higher release of encapsulated protein within 24 h. Nanoparticles in neutral pH and under oxidative conditions showed small molecule release and swelling of otherwise intact nanparticles. Notably, cellular studies show absence of toxicity and efficient uptake of nanoparticles by macrophages followed by cytoplasmic release of ovalbumin. Future work will apply this system to inflammatory diseases.

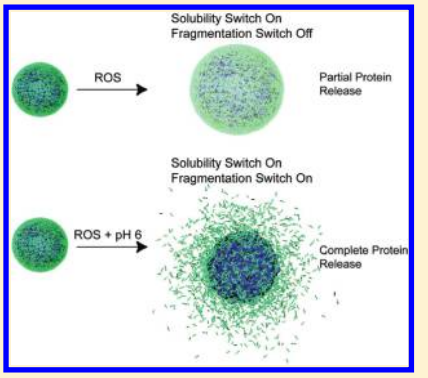

INTRODUCTION

Inflammation, especially chronic, relates to various diseases including cancerous and cardiovascular. Although there are numerous reports of "smart" nanoparticles that rapidly and selectively respond to different disease-specific stimuli, there is a dearth of nanoparticles capable of specifically targeting inflammation.[1,2] Furthermore, nanoparticles capable of cytoplasmic delivery are particularly challenging and this remains a major hurdle for effective therapeutic delivery.[3,4] In achieving increased cytoplasmic delivery, burst, fragmenting nanoparticles hold promise, as they can lead to elevated osmotic pressure within the endosome leading to endosomal escape of the nanoparticles payload.[5−7] Important biomarkers of diseased tissue that have been successfully used to trigger nanoparticle degradation include reduced extracellular pH,[8] thermal responsiveness,[9] reductive microenvironments,[10] and oxidative stress.[11] These nanoparticles respond to a single disease stimulus. Furthermore, control over the degradation kinetics, and thus, the ON/OFF state of the system has been difficult to achieve. For example, polyketals have gained prominence as the choice of drug delivery nanoparticles owing to their rapid pH response.[12,13] Nanoparticles formulated from these polyketals degrade at acidic pH into acetone and other benign molecules, rapidly releasing the payload within to the cytoplasm.[14] However, a key drawback of these systems is that as hydrophobic polymeric nanoparticles their degradation rates are very slow (many days)[12,13,15] in acidic pH (pH 6−5) because of reduced water influx. Although a hydrophobic backbone is advantageous in formulating stable nanoparticles at physiological conditions, a hydrophilic backbone is needed to produce fast release in targeted tissue. On the other hand, a hydrophilic backbone often results in nanoparticles that are not stable in pH 7.4 for longer than a few hours.[16] Recently, we introduced logic gate nanoparticles that use dual response mechanisms to impart stability to the "OFF" state while maintaining a rapid degradation or a sharp "ON" state.[6] We demonstrated the ability of such particles to deliver their payload to the cytoplasm because of the rapid fragmentation of the nanoparticle.[14] Here, we apply this strategy to physiological cues of inflammatory diseases.[17−19] Our new nanoparticles composed of a dual stimuli and response polymeric backbone are stable in healthy physiological conditions, yet they are able to rapidly fragment in subcellular and diseased conditions. Rapid fragmentation is important for cytoplasmic release of the bioactive payload.

It is known that polyketals degrade via surface hydrolysis while polysuflides degrade via bulk erosion.[28,29] Herein, we designed a novel polythioether ketal by incorporating a thioether moiety in our polymer backbone; the thioether acts as a solubility switch that turns the polymer more hydrophilic when it becomes oxidized from a thioether into a sulfone. Sulfones are inherently

Received: March 18, 2011
Revised: June 17, 2011
Published: June 21, 2011

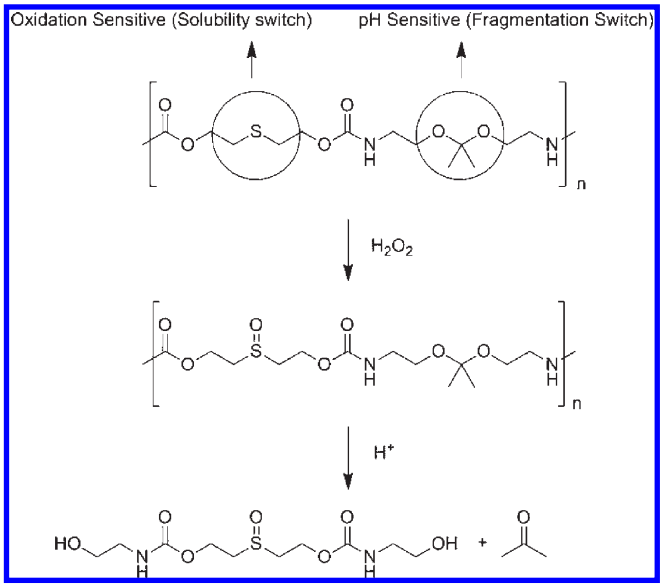

Figure 1. Degradation mechanism of polythioether ketal. Hydrogen peroxide and acidic pH stimulate the degradation of the polymeric nanoparticles in tandem.

more hydrophilic because of a strong dipole due to the presence of the sulfur oxygen double bond; this strong dipole leads to an increased affinity for water, resulting in an accelerated rate of hydrolysis of the ketal groups along the backbone. This allowed our polymers sharper, more rapid degradation kinetics in comparison to conventional polyketals (Figure 1). Various other polysulfides have been used to successfully formulate oxidation sensitive vesicles[1] and nanoparticles,[20] with such nanoparticles also being used to selectively target dendritic cells in vivo.[21]

The synthesized polythioether ketal nanoparticles were prepared to target the oxidative stress areas of many diseases including tumors,[22] atherosclerosis,[23] and causes of aging due to mitochondrial damage.[24] During these abnormalities, reactive oxygen species (ROS) are formed when oxygen undergoes a partial one-electron reduction to super oxide anion and subsequently forms hydrogen peroxide, hypochlorite peroxynitrite, and other oxidants.[25] Herein, the formulated nanoparticles that are triggered by both ROS and low pH (typical of inflamed tissue), function akin to an "AND" logic gate in circuits. We hope that our design will lead to nanoparticles that will better target diseased tissue for drug delivery or diagnostics.

MATERIALS AND METHODS

Materials. Potassium monohydrogen phosphate (K_2HPO_4) and potassium dihydrogen phosphate (KH_2PO_4) were purchased from Alfa Aesar Organics (Ward Hill, MA). Dichloromethane (DCM, methylene chloride) was purchased from Fisher Scientific (Hampton, NH). Nile red and poly(vinyl alcohol) (PVA) (MW 30−70k) were purchased from Sigma Chemical Co. (St. Louis, MO). 2,2′-Thiodiethanol was purchased Sigma Chemical Co. (St. Louis, MO). 4-Nitrophenylchloroformate was purchased from Acros organics (Belgium). PLGA (Resomer RG 502H) was purchased from Boehringer Ingelheim (Germany). Ovalbumin Alexa Fluor 594 was purchased from Invitrogen. All reagents were purchased from commercial sources and were used without further purification unless otherwise stated.

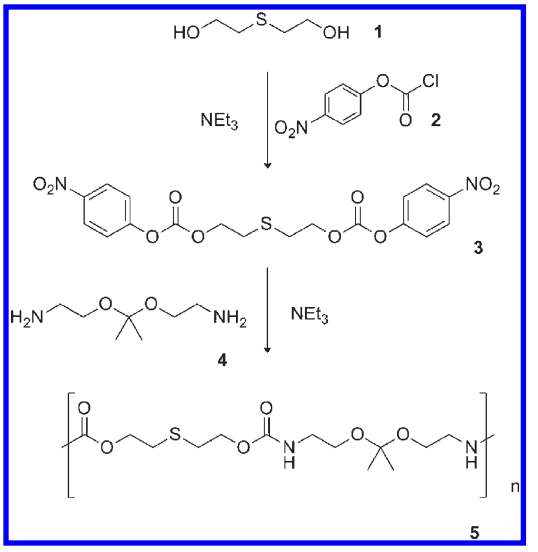

Figure 2. Synthesis of polythioether ketal.

Synthesis of the Polymer. As shown in Figure 2, 2,2′-thiodiethanol (compound **1**, 3.66 g, 0.03 mol) was taken with 4-nitrophenylchloroformate (compound **2**, 13.3 g, 0.064 mol) in a dry, round-bottom flask with 125 mL of dry dichloromethane and stirred under a nitrogen atmosphere. To this, triethylamine (30 mL, 0.21 mol) in 25 mL of dry dichloromethane was added dropwise over 30 min at room temperature. The reaction was subsequently stirred for 4 h. At the end of the reaction, the reaction mixture was rotavaped, diluted with 250 mL of dichloromethane, and extracted from 2 × 100 mL of 1% HCl. The organic layer was dried over $MgSO_4$ and rotavaped. The resulting crude solid was recrystallized from ethyl acetate three times to yield 8.0 g (0.017 mol, 60% yield) of a white solid (MP 138.6−140.1 °C).

^{1}H NMR (500 MHz, chloroform-*d*) δ 8.28 (d, J = 7.5 Hz, 1H), 7.38 (d, J = 7.5 Hz, 1H), 4.47 (dd, J = 6.3, 5.3 Hz, 1H), 2.97 (dd, J = 6.4, 5.2 Hz, 1H). ^{13}C NMR (126 MHz, chloroform-*d*) δ 155.46, 152.52, 145.61, 125.48, 121.91, 67.84, 30.79. HR-ESI-FT-MS (Orbit-Trap-MS) C18 H16 N2 O10 S Na. Mass Measured: 475.0420, Theo. Mass: 475.0418 δ (ppm) 0.4.

Polymer synthesis was completed by preparing diamine (compound **4**, Figure 2) as per the literature.[12] Diamine (0.518 g, 3.2 mmol) and carbonate (compound **3**, Figure 2) (1.446 g, 3.2 mmol) were taken with 2 mL of dry dichloromethane in an 8 mL vial with a Teflon cap and purged with nitrogen. To this, 1 mL of triethylamine was added via syringe, and the contents were stirred for 4 days at room temperature. The contents were precipitated into diethyl ether and the waxy yellow solid obtained was subsequently purified on a gel column packed with lipophilic sephadex (LH-20) using dichloromethane as the eluent, to obtain a pale yellow solid in 70% yield.

^{1}H NMR (500 MHz, chloroform-*d*) δ 5.42 (s, 1H), 4.21 (t, J = 6.4 Hz, 2H), 3.45 (t, J = 5.2 Hz, 2H), 3.30 (d, J = 5.3 Hz, 2H), 2.77 (t, J = 6.5 Hz, 2H), 1.32 (s, 3H). ^{13}C NMR (126 MHz, chloroform-*d*) δ 156.42, 100.32, 64.24, 64.21, 59.93, 41.20, 31.34, 24.93, 24.90. Molecular weight: Obtained via GPC against polystyrene standards using DMF(0.01% LiBr) as the eluent. M_w = 59 800 Da, M_n = 34 100, PDI = 1.75.

Nanoparticle Formulation. In o/w procedure, 25 mg of the synthesized polymer was dissolved in 2.5 mL DCM. Then,

500 μg Nile red were added, for preparing Nile red containing particles. DCM was added to 50 mL of phosphate buffer (pH 8) containing 1% PVA, and the mixture was stirred at 1000 rpm for 5 min to prepare an emulsion. Further emulsification was achieved using a high-pressure homogenizer (Microfluidic 110PS, USA) at 23 000 psi for three cycles. The nanoparticle suspension was stirred at 1000 rpm using a magnetic stirrer to evaporate the DCM. Nile red containing nanoparticles were filtered through 1 μm filter to remove the insoluble Nile red aggregate, and a concentrated mode tangential flow filtration system with 500 kDa Pellicon XL cassettes (Millipore, USA) was used to remove the PVA and any unencapsulated material. The nanoparticle suspension was concentrated to 10 mL and washed twice.[26] Protein was encapsulated into the nanoparticles using the w/o/w emulsion method. Briefly, 2 mg Ovalbumin Alexa Fluor 594 was dissolved in 0.2 mL of PBS buffer and subsequently emulsified with 5 mL of DCM containing 100 mg polymer using probe sonication (stabilized using 2% Span 80) at amplitude of 40% for 5 min (1/8 inch tip, Misonix S-4000, USA). The primary emulsion was added to 50 mL of 1% PVA in buffer (pH 8) under stirring at 1000 rpm, and the secondary emulsion was produced. Additional emulsification was achieved using the high-pressure homogenizer at 23 000 Psi for two cycles and tangential flow filtration was accomplished as previously described. Finally, 5% Trehalose was added to the particles before lyophilization. The lyophilized particles were suspended in aqueous media at different pHs and H_2O_2 levels for further evaluation of stability or release.

The encapsulation efficiencies of the particles were determined by incubating them at acidic pH in presence of 100 mM H_2O_2 until no further particles are detected by the DLS and the detected fluorescence reaches its maximum.

Dynamic Light Scattering Measurements of the Nanoparticles. Nanoparticles were suspended in a phosphate buffer pH 7.4 or 5 in the presence or absence 100 mM H_2O_2, with stability determined by monitoring their size for 24 h via dynamic light scattering (DLS) using a Zetasizer-ZS (fixed attenuator of 7, Malvern Worcestershire, UK).

Effect of pH and H_2O_2 on Nile Red Release. Nile red was encapsulated into the nanoparticles as a sensor of changes in the hydrophobic−hydrophilic character of the surrounding environment. Nile red fluoresces in the hydrophobic environment inside the nanoparticles and quenches once released into the aqueous release media; this quenching was measured as an indicator of Nile red release into an aqueous media. Nanoparticle powder was dispersed in PB pH 7.4 or 5 in the presence or absence 100 mM H_2O_2. The pH was checked in the presence of H_2O_2 to confirm the pH. Samples were taken and Nile red fluorescence was determined at different time intervals. Decrease in the nanoparticles fluorescent was an indication of Nile red release to the aqueous media.

Effect of pH and H_2O_2 on Ovalbumin Release. Nanoparticle powder was dispersed in PB pH 7.4 or 6.5 in presence or absence 100 mM H_2O_2. PB pH 6.5 was chosen for ovalbumin release study to prevent its precipitation upon release into PB having pH near ovalbumin isoelectric point (pH ~5).[27] Samples were taken at different time intervals and spun down at 20K *g* for 10 min at 4 °C. The supernatant was analyzed for released ovalbumin Alexa Fluor 594 after appropriate dilution.

Degradation of the Polythioether Ketal by ^{1}H NMR. Ten milligrams of the polymer were taken with deuterated (a) 1:1 acetonitrile−water (pH = 5, phosphate buffer); (b) 1:1 acetonitrile−water (pH = 5, phosphate buffer) with 20 μL of H_2O_2; the ^{1}H NMR was obtained at regular intervals.

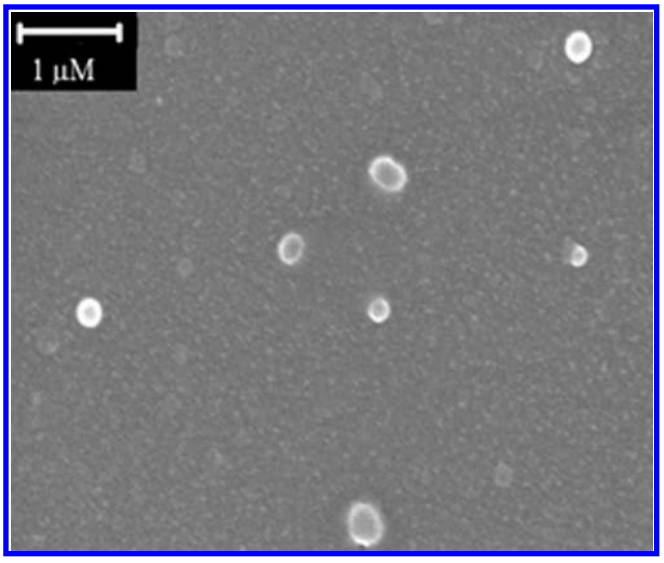

Figure 3. SEM image of the nanoparticles showing a particle diameter of <1 μm.

Cell Toxicity of Nanoparticles. The cytotoxicity of nanoparticles was investigated using a 3-(4,5-dimethylthiazol-2-yl)-2,5-diphenyltetrazolium bromide (MTT) reduction assay. RAW 264.7 macrophage cells were seeded at a density of 15 000 cells/well in a 96-well plate and incubated for 24 h to reach 60% confluency. Cells were treated with various amounts of nanoparticles that corresponded to the varying amounts of polymer contained in them (0−300 μg/mL) and incubated for 20 h. To each well was added 10 μL of MTT solution, and the wells were incubated for 3 h. Dimethyl sulfoxide (DMSO, 100 μL) was added to cells to dissolve the resulting formazan crystals. After 20 min of incubation, the absorbance at 570 nm was measured using a FlexStation microplate reader (Molecular Devices, Inc., Sunnyvale, CA, USA). Cell viability was obtained by comparing the absorbance of nanoparticle-treated cells to that of control cells not treated with particles.

Cellular Internalization of Ovalbumin-Containing Nanoparticles. The uptake of ovalbumin Alexa Fluor 594-loaded nanoparticles was studied in RAW264.7 cells using a fluorescent microscope. Cells were plated on CultureWell Chambered Coverglass slides (Invitrogen Corporation, Carlsbad, CA, USA) at a density of 10 000 cells per well for 24 h followed by treatment with polythioketal or PLGA nanoparticles. The nanoparticle payload contained a final concentration of approximately 10 μg/mL ovalbumin Alexa Fluor594. After 8 h at 37 °C, the cells were washed with PBS before mounting and staining with DAPI.

RESULTS AND DISCUSSION

Infected tissues are frequently characterized by a decreased pH and the presence of reactive oxygen species (ROS).[17−19] In order to simulate these conditions, particle behavior was tested at acidic pH and in the presence of H_2O_2, which is a prevalent reactive oxygen species. Accordingly, nanoparticles were subjected to different physiologically relevant conditions: pH 7.4 (pH of healthy tissue), pH 7.4/100 mM H_2O_2 (presence of ROS), acidic pH, and acidic pH/100 mM H_2O_2. Their behavior was

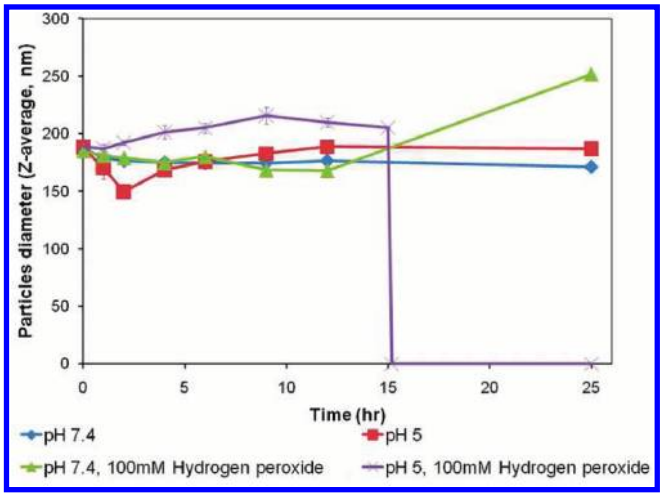

Figure 4. Effect of pH and H_2O_2 on the *Z*-average of the nanoparticles. Triplicate measurements were taken using the DLS at a fixed attenuator of 7.

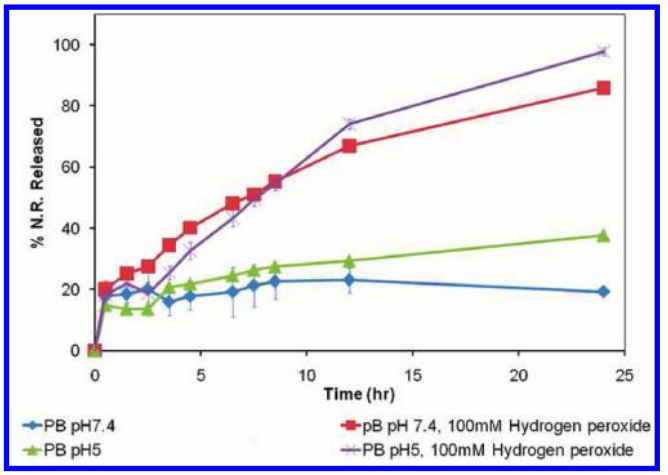

Figure 5. Release of Nile red from polythioether ketal nanoparticles. Decrease in nanoparticle suspension fluorescence was correlated to Nile red release in different conditions.

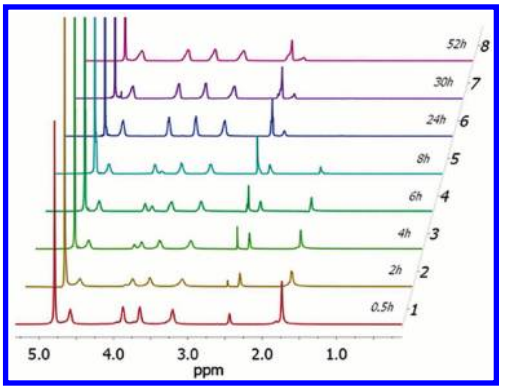

Figure 6. Degradation of polymer 5 at pH 5 in 1:1 deuterated acetonitrile and water by ^{1}H NMR. Hydrolysis of ketal is evidenced by the appearance of acetone peak (at δ 2.6 ppm) and disappearance of the ketal peak (at δ 1.6 ppm). There is also a concomitant change in the peak at δ 3.8 ppm to δ 3.9 ppm due to the formation of alcohol upon degradation of the ketal.

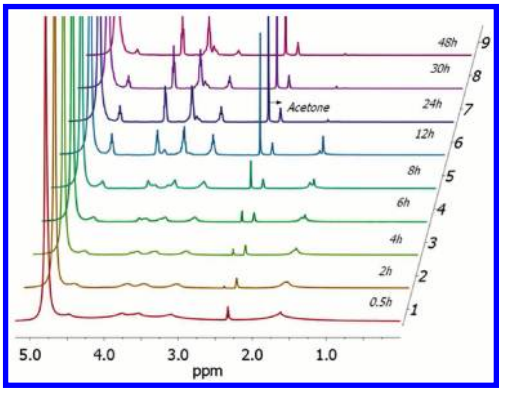

Figure 7. Degradation of polymer 5 at pH 5 in 1:1 deuterated acetonitrile and water with addition of 20 μL of 30% H_2O_2 by ^{1}H NMR. In addition to the changes noted in the Figure 6, upon addition of H_2O_2 we see that the peak at δ 3.6 ppm shifts to δ 3.7 ppm. This is consistent with the oxidation of sulfur in the backbone to a sulfoxide. These NMR studies establish that the sulfur moiety undergoes oxidation when subjected to H_2O_2.

monitored via DLS and by measuring the release of Nile red and ovalbumin.

The hydrophobic nature of the polymer permitted the formulation of the nanoparticles using single- or double-emulsion techniques. This in turn allowed the encapsulation of different payloads with different hydrophobic−hydrophilic characteristics like Nile red and ovalbumin (Figure 3).

Monitoring the behavior of the nanoparticles using DLS (Figure 4) showed that only nanoparticles dispersed in pH 5 in the presence of H_2O_2 degraded within 24 h, while the particles dispersed in pH 5 alone remained detectable throughout this time period. Thus, the presence of both stimuli caused an accelerated degradation of the nanoparticles. This is further evidenced by the observed increase in particle size upon incubation in H_2O_2 at pH 7.4. This swelling is due to the backbone becoming oxidized, resulting in the hydration of the particles.

When Nile Red is encapsulated in the particles, it acts as a fluorescent probe of hydrophobicity and release. In the presence of H_2O_2, oxidation of the polymer backbone occurs, rendering the nanoparticles more hydrophilic. This causes quenching of encapsulated Nile red upon its release from the nanoparticles (*Z*-average = 200 nm). This hydrophilic change occurred in both neutral and acidic conditions and depended entirely on whether the particles were incubated in hydrogen peroxide or not (Figure 5). Also, Nile red was minimally quenched at pH 5 due to the slow degradation of the particle via surface erosion. However, more quenching is observed when both conditions are operational. Finally, in order to confirm that our polymer degrades under the said conditions, we performed degradation and analyzed via ^{1}H NMR (Figure 6 and Figure 7). Here, as expected, we did not see a difference in polyketal hydrolysis rates because the polymer is completely dissolved without the need of oxidation. The control that we observed in the rates of particle degradation is due to the nanoparticle architecture, which is lost when the polymer is dissolved. We subsequently tested this systemic control in releasing ovalbumin as a model protein.

Figure 8 shows that ovalbumin release was initiated by oxidation of the polymer, or more accurately due to *swelling* of the nanoparticles. Meanwhile, higher release was observed at acidic pH in the presence of hydrogen peroxide due to

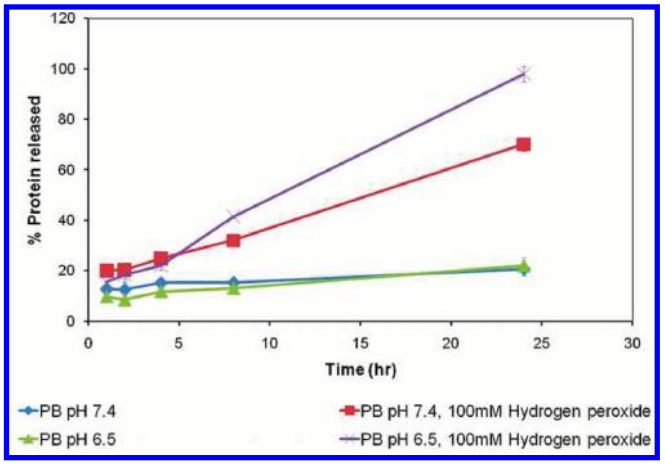

Figure 8. Release of ovalbumin AlexaFluor 488 from polythioketal nanoparticles. Nanoparticle supernatants were tested for fluorescence to determine ovalbumin release profile over time (n = 3).

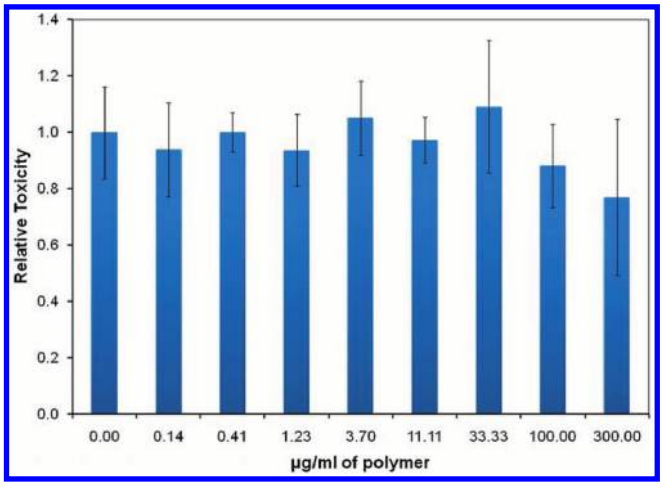

Figure 9. Cytotoxicity of polythioether ketal nanoparticles at different concentrations in RAW 264.7 macrophage cells. The cells were incubated with the nanoparticles for 20 h before performing the MTT assay.

degradation of the nanoparticles. Importantly, the nanoparticles showed excellent stability at pH 7.4. Furthermore, the full degradation of our new nanoparticles system is important as small fragments are more readily excreted.[30−32]

We evaluated the cytotoxicity of polythioketal nanoparticles in cells using the MTT assay using RAW264.7 cell line. The RAW264.7 macrophage cell line is a great model system for studying immune response and can produce relatively higher levels of endogenous ROS. Additionally, these cells are able to take up cells very readily without the need of cell penetrating peptides.

RAW 264.7 cells were incubated with various amounts of nanoparticles for 20 h. Figure 9 illustrates the comparison of cytotoxicity between cells treated with increasing concentrations of polythioether ketal polymer. There was no significant cytotoxicity observed with the cells incubated with up 300 μg/mL of polymer (p = 0.294).

Finally, we analyzed the cellular uptake of nanoparticles and release of cargo within cells by comparing polythioether ketal and PLGA nanoparticles containing equal amounts of fluorescently

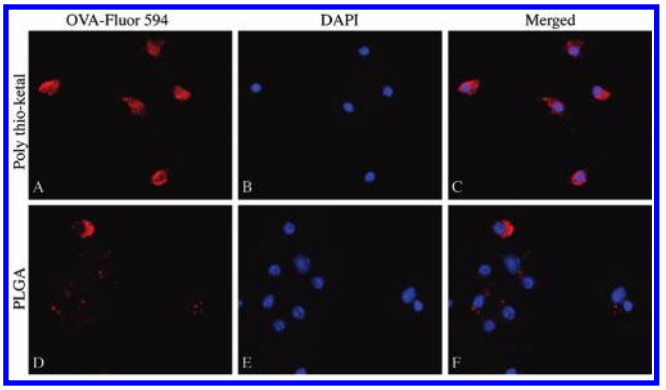

Figure 10. Uptake of nanoparticles loaded with fluorescent ovalbumin. Raw 264.7 macrophage cells were treated for 8 h with polythioether ketal or PLGA nanoparticles containing ovalbumin Alexa Fluor 594 (red) and stained with DAPI (blue).

labeled ovalbumin (Figure 10). Nanoparticles were added to RAW 264.7 cells and evaluated by fluorescence microscopy. Polythioether ketal nanoparticles were able to efficiently deliver protein within RAW264.7 macrophage cells that have an H_2O_2 concentration of 2 μM.[33]

Cells treated with polythioether ketal nanoparticles show thorough diffusion of ovalbumin throughout the cytoplasm and the nucleus, indicating that labeled ovalbumin was released within the cell. This is in contrast to slow-degrading PLGA nanoparticles that show punctuated spots and less diffused ovalbumin throughout the cell.

CONCLUSION

We designed a polymeric nanoparticle with two stimuli responsive moieties in its backbone, and which undergoes programmed degradation when stimulated by inflammatory cues, ROS, and acidic pH, respectively. This system functions akin to an "AND" Logic Gate. Upon stimulation by ROS, the polymer becomes hydrophilic, followed by ketal hydrolysis promoted at an acidic pH. We observed release of small hydrophobic molecules, Nile red, in acidic pH and an increase in polymer hydrophilicity upon oxidation. Higher release of encapsulated ovalbumin was observed in the presence of both hydrogen peroxide and acidic pH. We found that the nanoparticles were readily taken up by macrophage cells and that ovalbumin release from the nanoparticles into the cytoplasm was in agreement with the degradation behavior of the nanoparticles as shown in the DLS measurements. We hypothesize that these nanoparticles can differentiate among the conditions of our target areas from others. This should ensure the release of the payload in specific diseased regions such as inflammatory or tumor sites and allows for intracellular delivery. These studies suggest that our nanoparticles can be applied to the delivery of diagnostics and therapeutics to sites of inflammation. Thus, our current work focuses on the application of these nanoparticles in targeting theranostics to vulnerable plague versus stable plaque.

ASSOCIATED CONTENT

Supporting Information. ^{1}H NMR of compound **3**, ^{13}C NMR of compound **3**, HR-ESI-FT-MS (Orbit-Trap-MS) of compound **3**, ^{1}H NMR of *poly* 5, ^{13}C NMR of *poly* 5, GPC trace

of Poly 5 calibrated against Polystyrene standards. This material is available free of charge via the Internet at http://pubs.acs.org.

AUTHOR INFORMATION

Corresponding Author
*Prof. Adah Almutairi, aalmutairi@ucsd.edu.

ACKNOWLEDGMENT

The research described in this paper was sponsored in part by the UCSD IRACDA Fellowship NIH Grant GM06852 (JM), the NIH New Innovator Award (1 DP2 OD006499-01), and the King Abdulaziz City for Science and Technology (KACST). We thank Dr. Eric Schopf for his help with SEM imaging.

REFERENCES

(1) Napoli, A., Valentini, M., Tirelli, N., Mueller, M., and Hubbell, J. A. (2004) Oxidation-responsive polymeric vesicles. *Nat. Mater. 3*, 183–189.

(2) Wilson, D. S., Dalmasso, G., Wang, L. X., Sitaraman, S. V., Merlin, D., and Murthy, N. (2010) Orally delivered thioketal nanoparticles loaded with TNF-alpha-siRNA target inflammation and inhibit gene expression in the intestines. *Nat. Mater. 9*, 923–928.

(3) Vasir, J. K., and Labhasetwar, V. (2007) Biodegradable nanoparticles for cytosolic delivery of therapeutics. *Adv. Drug Delivery Rev. 59*, 718–728.

(4) Mescalchin, A., Detzer, A., Wecke, M., Overhoff, M., Wuensche, W., and Sczakiel, G. (2007) Cellular uptake and intracellular release are major obstacles to the therapeutic application of siRNA: novel options by phosphorothioate-stimulated delivery. *Expert Opin. Biol. Ther. 7*, 1531–1538.

(5) Hu, Y., Litwin, T., Nagaraja, A. R., Kwong, B., Katz, J., Watson, N., and Irvine, D. J. (2007) Cytosolic delivery of membrane-impermeable molecules in dendritic cells using pH-responsive core-shell nanoparticles. *Nano Lett. 7*, 3056–3064.

(6) Sankaranarayanan, J., Mahmoud, E. A., Kim, G., Morachis, J. M., and Almutairi, A. (2010) Multiresponse strategies to modulate burst degradation and release from nanoparticles. *ACS Nano 4*, 5930–5936.

(7) Sonawane, N. D., Szoka, F. C., Jr., and Verkman, A. S. (2003) Chloride accumulation and swelling in endosomes enhances DNA transfer by polyamine-DNA polyplexes. *J. Biol. Chem. 278*, 44826–44831.

(8) Vaupel, P., Kallinowski, F., and Okunieff, P. (1989) Blood flow, oxygen and nutrient supply, and metabolic microenvironment of human tumors: a review. *Cancer Res. 49*, 6449–65.

(9) Meyer, D. E., Shin, B. C., Kong, G. A., Dewhirst, M. W., and Chilkoti, A. (2001) Drug targeting using thermally responsive polymers and local hyperthermia. *J. Controlled Release 74*, 213–224.

(10) Saito, G., Swanson, J. A., and Lee, K.-D. (2003) Drug delivery strategy utilizing conjugation via reversible disulfide linkages: role and site of cellular reducing activities. *Adv. Drug Delivery Rev. 55*, 199–215.

(11) Vo, C. D., Kilcher, G., and Tirelli, N. (2009) Polymers and sulfur: what are organic polysulfides good for? Preparative strategies and biological applications. *Macromol. Rapid Commun. 30*, 299–315.

(12) Paramonov, S. E., Bachelder, E. M., Beaudette, T. T., Standley, S. M., Lee, C. C., Dashe, J., and Frechet, J. M. J. (2008) Fully acid-degradable biocompatible polyacetal microparticles for drug delivery. *Bioconjugate Chem. 19*, 911–919.

(13) Heffernan Michael, J., and Murthy, N. (2005) Polyketal nanoparticles: a new pH-sensitive biodegradable drug delivery vehicle. *Bioconjugate Chem. 16*, 1340–2.

(14) Broaders, K. E., Cohen, J. A., Beaudette, T. T., Bachelder, E. M., and Frechet, J. M. J. (2009) Acetalated dextran is a chemically and biologically tunable material for particulate immunotherapy. *Proc. Natl. Acad. Sci. U. S. A. 106*, 5497–5502.

(15) Jain, R., Standley, S. M., and Frechet, J. M. J. (2007) Synthesis and degradation of pH-sensitive linear poly(amidoamine)s. *Macromolecules 40*, 452–457.

(16) Murthy, N., Thng, Y. X., Schuck, S., Xu, M. C., and Frechet, J. M. J. (2002) A novel strategy for encapsulation and release of proteins: Hydrogels and microgels with acid-labile acetal cross-linkers. *J. Am. Chem. Soc. 124*, 12398–12399.

(17) Punnia-Moorthy, A. (1987) Evaluation of pH changes in inflammation of the subcutaneous air pouch lining in the rat, induced by carrageenan, dextran and staphylococcus aureus. *J. Oral Pathol. Med. 16*, 36–44.

(18) Ródenas, J., Mitjavila, M. T., and Carbonell, T. (1995) Simultaneous generation of nitric oxide and superoxide by inflammatory cells in rats. *Free Radical Biol. Med. 18*, 869–875.

(19) Greenwald, R. A. (1991) Oxygen radicals, inflammation, and arthritis: Pathophysiological considerations and implications for treatment. *Seminars in Arthritis and Rheumatism 20*, 219–240.

(20) Rehor, A., Hubbell, J. A., and Tirelli, N. (2005) Oxidation-sensitive polymeric nanoparticles. *Langmuir 21*, 411–417.

(21) Reddy, S. T., Rehor, A., Schmoekel, H. G., Hubbell, J. A., and Swartz, M. A. (2006) In vivo targeting of dendritic cells in lymph nodes with poly(propylene sulfide) nanoparticles. *J. Controlled Release 112*, 26–34.

(22) Giles, G. I. (2006) The redox regulation of thiol dependent signaling pathways in cancer. *Curr. Pharm. Des. 12*, 4427–4443.

(23) Navab, M., Ananthramaiah, G. M., Reddy, S. T., Van Lenten, B. J., Ansell, B. J., Fonarow, G. C., Vahabzadeh, K., Hama, S., Hough, G., Kamranpour, N., Berliner, J. A., Lusis, A. J., and Fogelman, A. M. (2004) Thematic review series: The pathogenesis of atherosclerosis: The oxidation hypothesis of atherogenesis: The role of oxidized phospholipids and HDL. *J. Lipid Res. 45*, 993–1007.

(24) Shigenaga, M. K., Hagen, T. M., and Ames, B. N. (1994) Oxidative damage and mitochondrial decay in aging. *Proc. Natl. Acad. Sci. U. S. A. 91*, 10771–8.

(25) Szatrowski, T. P., and Nathan, C. F. (1991) Production of large amounts of hydrogen peroxide by human tumor cells. *Cancer Res. 51*, 794–798.

(26) Dalwadi, G., Benson, H. A., and Chen, Y. (2005) Comparison of diafiltration and tangential flow filtration for purification of nanoparticle suspensions. *Pharm. Res. 22*, 2152–62.

(27) Smith, E. R. B. (1935) The effect of variations in ionic strength on the apparent isoelectric point of egg albumin. *J. Biol. Chem. 108*, 187–194.

(28) Khutoryanskiy, V. V., and Tirelli, N. (2008) Oxidation-responsiveness of nanomaterials for targeting inflammatory reactions. *Pure Appl. Chem. 80*, 1703–1718.

(29) Burkersroda, F. v., and Goepferich, A. M. (1999) An approach to classify degradable polymers. *Mater. Res. Soc. Symp. Proc. 550*, 17–22.

(30) Greish, K., Fang, J., Inutsuka, T., Nagamitsu, A., and Maeda, H. (2003) Macromolecular therapeutics - Advantages and prospects with special emphasis on solid tumour targeting. *Clin. Pharmacokinetics 42*, 1089–1105.

(31) Kwon, G. S., Yokoyama, M., Okano, T., Sakurai, Y., and Kataoka, K. (1993) Biodistribution of micelle-forming polymer drug conjugates. *Pharm. Res. 10*, 970–974.

(32) Lu, Z. R., Parker, D. L., Goodrich, K. C., Wang, X. H., Dalle, J. G., and Buswell, H. R. (2004) Extracellular biodegradable macromolecular gadolinium(III) complexes for MRI. *Magn. Reson. Med. 51*, 27–34.

(33) Gong, X., Li, Q., Xu, K., Liu, X., Li, H., Chen, Z., Tong, L., Tang, B., and Zhong, H. (2009) A new route for simple and rapid determination of hydrogen peroxide in RAW264.7 macrophages by microchip electrophoresis. *Electrophoresis 30*, 1983–1990.